USING ACTIVATED CARBON DERIVED FROM COCONUT FIBER TO REMOVE CHROMIUM (VI)

● DANG VIET HUNG

ABSTRACT:

Biochar is considered an economical adsorption medium because of its capacity to remove heavy metals and organic pollutants from polluted water. In this work, phosphoric acid (H_3PO_4) was used in a unique manner to promote the production of coconut fiber activated carbon (AC) from biochar carbon (BC) by pyrolysis. The resulting product was then tested for effective adsorption of Cr (VI) from aqueous environments. To evaluate the structure and content of BC and AC, advanced characterization techniques such as SEM, EDS, and pH_{pzc} were used. Compared to the BC's removal rate of 38.5%, the AC was able to remove 48.05% of Cr(VI). The following factors had a significant impact on the rate of Cr(VI) removal: temperature, kinetics, isotherm, adsorption time, pH, and adsorption capacity. The adsorption curve of AC matches well with the pseudo-second-order kinetic model.

Keywords: Cr(VI) removal, activated carbon, coconut fiber, adsorption, phosphoric acid.

1. Introduction

Chromium is a highly poisonous and carcinogenic element that is mostly released into soil and water streams by industrial waste, endangering living things [1]. The crust of the planet contains large concentrations of the heavy metal Cr. Cr exists in the following oxidation states: −2, −1, 0, +1, +2, +3, +4, +5, and +6, the most stable of which are the +3 and +6 oxidation states in the environment [2]. Pollutant chromium is non-biodegradable and spreads via various pathways into the food chain. Due to its extreme toxicity, it is included as one of the top 20 pollutants on the list of dangerous compounds [3]. Whereas the average amounts of Cr in surface water, rainwater, groundwater, and seawater are 0.2–1 μg/L, 0.5–2 μg/L, and 0.04–0.5 μg/L respectively [4]. The WHO recommends 0.1 mg/L as the maximum contamination level for Cr in drinking water. High levels of Cr were found in the blood, urine, placental tissue, and umbilical cord of workers in the chromium industry [5]. Abortions, irregular menstruation, and deformed babies were also documented [6]. While human hosts have several defense mechanisms to counteract the harm produced by reactive oxygen species, chronic exposure to Cr(VI) compromises human defense mechanisms [7, 8].

The first known adsorbent is AC, which has a huge internal surface area, a highly porous

structure, and good adsorption capabilities for a variety of compounds [9, 10]. The need for AC in industry is great and continues to rise, as does the amount produced. The majority of AC is produced using non-renewable coal-based resources (around 80% - 85%), with the remainder coming from renewable sources like wood, coconut shells, and agricultural leftovers [11, 12]. Lignin can satisfy the high carbon yield criterion for the commercial manufacturing of AC because it is a hydrocarbon macromolecule with a carbon content of more than 60% [13]. The preparation of ACs can be done in two ways: chemically and physically. However, compared to physical activation, chemical activation has demonstrated better benefits for creating ACs with a greater yield and surface area at moderate temperatures in just one step [14]. Chemical activation agents that are most frequently utilized are $ZnCl_2$, H_3PO_4, and alkali metal complexes (NaOH, KOH, Na_2CO_3, and K_2CO_3) [15-17]. High temperatures of 600–900°C are frequently used to process alkali, such as KOH, with an impregnation ratio (IR = carbon biomass:catalyst) of 1:2–5 [18]. Nevertheless, KOH activation has a low carbon yield and is harmful to the environment and human health [19]. Conversely, H_3PO_4 has a low IR of 1:1–3, making it useful at low temperatures of 400–600°C [20]. Using H_3PO_4 as a catalyst not only encourages bond cleavage reactions but also helps create a layer of linkage through condensation, cyclization, and the formation of phosphate and polyphosphate esters, which may shield the internal pore structure and limit excessive burn-off during carbon activation [21]. In the last few decades, H_3PO_4 has been utilized more frequently in large-scale AC production due to its high attractiveness when it comes to energy cost, carbon yield, and environmental impact [22]. According to these findings, phosphoric acid can effectively increase the pore size and specific surface area of biochar while also improving the adsorption of other ions on the surface area of the functional groups, indicating that it is a useful chemical activator for improving biochar adsorption [23]. Prior research concentrated on modifying biochar under ideal circumstances to increase its adsorption capacity. Few have documented their efficacy at varying pH ranges. It is necessary to examine the effectiveness of acid-modified biochar at various pH ranges as well as the effects of dose, duration, and temperature on chromium remediation.

For the creation of biochar, the coconut fiber from the coconut processing factory in Vietnam was gathered using coconut fiber. Thermal decomposition was used to create activated carbon (AC) from coconut fiber, and the properties of eucalyptus biological carbon were examined both before and after modification [24]. In order to increase the surface area of the biochar, coconut fiber activated carbon was created by pyrolyzing the BC after it had been chemically activated with H_3PO_4. Chemical activation can be used to change the characteristics of biochar either before or after carbonization. In order to identify the ideal adsorption conditions, this study sought to ascertain the effects of adsorbent quantity, pH, and adsorption period on the adsorption performance of modified biochar. Additionally, batch adsorption studies on the isotherms, thermodynamics, and adsorption kinetics of Cr(VI) in an aqueous environment will be used to determine the behavior and mechanism of adsorption. This work offers a trustworthy research design and a point of reference for the bio-carbon surface modification of coconut fiber.

2. Materials and methods

2.1. Chemical

Alpha Chemical Reagent Co., Ltd. (Tianjin, China) provided the potassium dichromate ($K_2Cr_2O_7$), sodium hydroxide (NaOH), hydrochloric acid (HCl), acid phosphoric (H_3PO_4), and 1,5 Diphenylcarbazide used in this investigation, all of which met the criteria for analytical grade. Chemicals were diluted in deionized water to provide working solutions for every experiment.

2.2. Preparation of adsorbents

Coconut fiber was collected from coconut processing factories in Vietnam. The material derived from coconut fiber was expected to be exceptionally fine in size. It was firstly dried at 105°C for 24 h and sieved to obtain a size range of 0.250 mm for storage. Next, the production was taken and pyrolyzed in a muffle furnace at 700°C for 2 h with a ramping rate of 10 C/min. The acquired eucalyptus charcoal was washed thrice with deionized water and subjected to solid-liquid separation using centrifugation and dried at 75°C in an oven for 24 h to get coconut fiber biochar carbon (BC), which was sealed and stored then. The coconut fiber activated carbon (AC) derived from BC was prepared by activating BC using H_3PO_4. Briefly, BC mixed phosphoric acid (40%) solution of a 1:3 ratio was placed in a beaker, sealed with parafilm, and impregnation for 24h, and the immersed enamel was prepared. The carbon was pyrolyzed in a muffle furnace at 600°C for 2 h, and the temperature was gradually raised at a rate of 10°C/min. The BC was then rinsed with deionized water and centrifuged for solid-liquid separation, repeating the operation several times. Separated by a Buchner funnel, the coconut fiber material was placed in an oven at 75°C for 24 h, to obtain coconut fiber activated carbon (AC), which was sealed for subsequent experiments.

2.3. Batch adsorption studies

The adsorption experiments were conducted in batch reactor with the solid/liquid ratio of 2.0 g/L in a thermostatic shaker. The appropriate concentration of Cr(VI) solution was obtained by dissolving $K_2Cr_2O_7$ in DI water. The diphenylcarbazide method was used to measure the concentration of Cr (VI) after and before the adsorption process. Diphenylcarbazide forms a red-violet complex with Cr(VI), and the intensity of this complex was detected at 540 nm with a UV–vis spectrophotometer (Hitachi U-2910, Hitachi Corp. Japan). Cr(VI) concentrations were determined and adsorption capacity was calculated by Eq. (1) and removal of Cr(VI) was calculated by Eq. (2) at defined time intervals until reaching adsorption equilibrium after samples being taken and filtrated through a 0.45-mm WhatmanR membrane filter.

$$q_e = \frac{(C_0 - C_e) \times V}{\mathrm{m}} \qquad (1)$$

$$Re = \frac{(C_0 - C_e) \times 100}{C_0} \qquad (2)$$

where:

C_e (mg/L) is the Cr(VI) concentration at equilibrium;

C_0 (mg/L) is the initial concentration of Cr(VI);

q_e (mg/g) is the adsorption capacity at equilibrium;

V (L) is the volume of Cr(VI) solution;

m (g) is the mass of the adsorbent.

In the optimum pH adsorption experiment, 0.2 g BC and AC were added into 100 mL centrifuge tube, and 100 mL of 50 mg/L hexavalent chromium solution by adjusting pH to 2, 3, 4, 5, 6, 7, and 8 at room temperature of 35°C. Then it was placed in a fixed temperature air bath oscillator at a speed of 150 r/min at 35°C and shaken for 24 h. The sample was removed to measure Cr(VI) concentration. The optimal dosage of 0.5 g/L, 1.0 g/L, 1.5 g/L, 2.0 g/L, 2.5 g/L, 3.0 g/L BC and AC were taken at 35°C, following the addition of 100 mL hexavalent chromium solution (50 mg/L) at pH 2. The sample was placed in a fixed temperature air bath oscillator at a speed of 150 r/min at 35°C and shaken for 24 h. The Cr(VI) determination method is the same as mentioned above. The optimum reaction time was obtained by using three kinds of hexavalent Cr(VI) solutions. 100 mL of Cr(VI) solutions with heavy metal dosages 50 mg/L, 100 mg/L, 200 mg/L, 300 mg/L, 400 mg/L, and 500 mg/L were chosen by adjusting pH to 2 at room temperature of 35°C, and were oscillated from 0 to 180 min at a speed of 150 r/min, respectively. Cr(VI) concentration is determined by the method mentioned above. Sorption isotherms were performed in the environment of 25°C, 35 oC, and 45°C, BC and AC with 0.2 g were placed in 100 mL centrifuge tubes.

Then 100 mL varying Cr(VI) solutions were added (dosages 50 mg/L, 100 mg/L, 200 mg/L, 300 mg/L, 400 mg/L, and 500 mg/L, respectively) into centrifuge tubes with a pH of 2.0 and placed on a shaker.

2.4. Characterization of adsorbents

The surface morphology of materials and main surface elements was presented in the scanning electron microscope (SEM) images and the energy dispersive X-ray spectroscopy (EDS) data (JSM-6510 LV), respectively. The drift method was used to calculate the pH value of the material's point zero charges (pH_{PZC})

3. Results and discussion

3.1. Characterization of materials

3.1.1. SEM-EDS

The SEM images of BC and AC are shown in Fig. 1. The particles in BC are primarily tiny and irregularly shaped, whereas the particles in AC are uniformly sized. Table 1 shows that the elemental composition of AC increased for oxygen (3.88%), declined for carbon (12.64%), and occupied 8.76 percent for P (phosphorus). This alteration may have been caused by the P element adhering to the O element during the modification procedure. The structural alterations on the AC surface seem to be mostly caused by the phosphorous attachment [25].

Table 1. Elemental composition of BC and AC materials

Adsorbent	Elemental content change		
	C (%)	O (%)	P (%)
BC	84.82	15.18	-
AC	72.18	19.06	8.76

Source: Analysis by author

3.1.2. pH_{pzc} analysis

One distinguishing feature of the electrical state of the adsorbent surfaces in solutions was the point of zero charges (PZC). The pH level at which the net (internal and external) surface charge of an adsorbent is zero is denoted by the value of pH_{PZC}. Fig. 2 displays the plot and pH_{PZC} values of adsorbent samples that were acquired by the pH drift method. The material pH_{PZC} values showed that the absorbent's pH_{PZC} values was significantly influenced by chemical agents, as seen by the order of AC (6.64).

Figure 1: SEM images of the porous structure characteristics: BC (a) and AC (b)

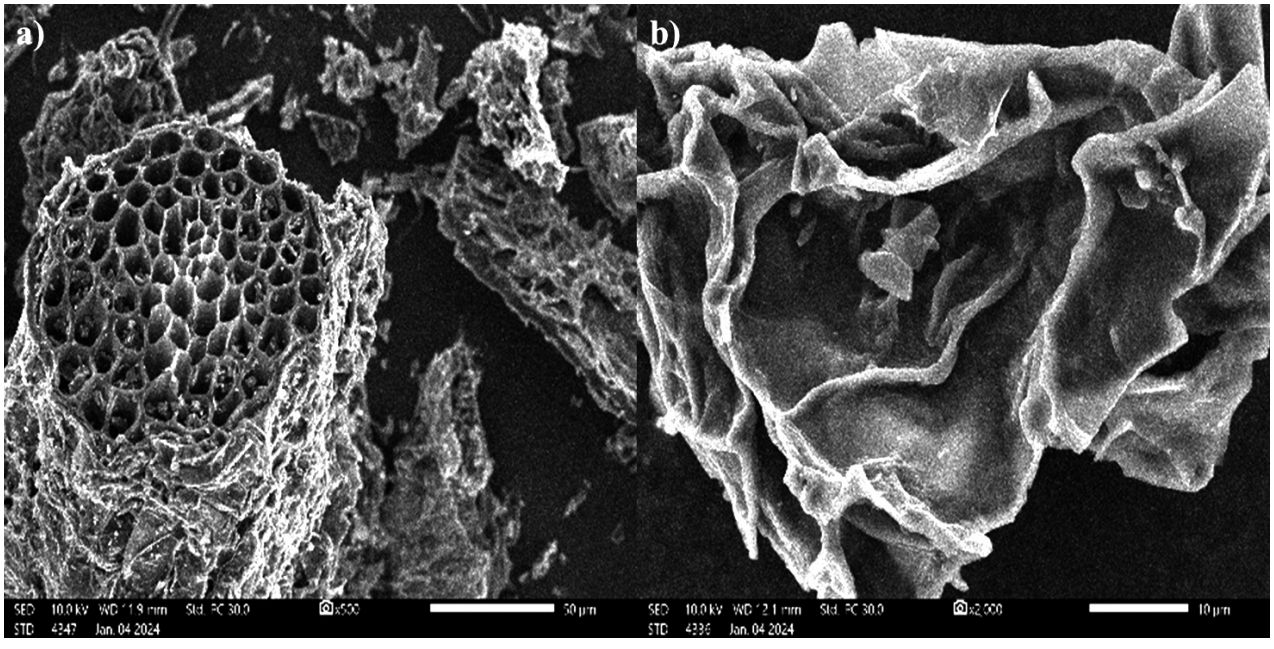

Source: Analysis by author

Figure 2: pH_{pzc} analysis of AC material

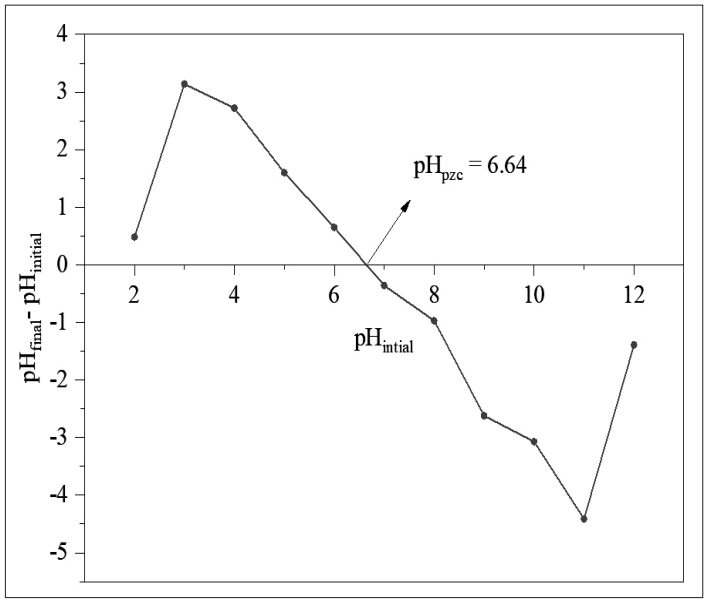

Source: Analysis by author

3.2. Effect of pH for Cr(VI) removal by adsorbents

The pH, which directly influences the presence of ions in an aqueous medium, is a significant component that influences the adsorption of metallic ions [26]. The adsorption of Cr(VI) by BC and AC under various pH values is shown in Fig. 3a. The maximum reached at pH 2 was 14.57 mg/g with a 48.50% clearance rate, which is 1.4 times greater than BC. The adsorption concentration dramatically drops as pH rises. Hexavalent chromium, or $HCrO_4^-$, is present in water at low pH values of 2, where the adsorbent surface is positive and electrostatic repulsion is weak [27]. On the other hand, as pH rose, the negative charge on the adsorbent surface increased, causing Cr(VI) to change into CrO_4^{2-} in water [28]. As presented in Fig. 2b, the pH_{PZC} of AC material is 6.64, implying that when solution pH decreases below these values, the surface of materials was more positively charged, and more electrostatic attraction occurs with negative ions (Cr(VI)) [29]. Therefore, the highest adsorption capacity of Cr(VI) onto the surface of adsorbents was found as the lowest pH value (pH 2) as demonstrated in Fig. 3a.

3.3. Effect of adsorbent dose; contracting time and temperature s for Cr(VI) removal by adsorbents

The adsorption of Cr(VI) by BC and AC at different adsorption dosages is shown in Fig. 3b. A progressive rise in Cr(VI) adsorption was noted along with the dosage increase. The little adsorbent dosage that hasn't been fully removed from the adsorption site to eliminate Cr(VI) is likely the cause of the steady decrease in the amount of adsorption per gram of the adsorbent. Consequently, the clearance rate is low and the adsorption amount per gram approaches its maximum value [30]. Long-term addition of the adsorbent resulted in the adsorption site reaching a supersaturation state, which decreased the amount of adsorbed Cr(VI) per gram of the adsorbent but increased the removal rate to a maximum [31].

Effect of contacting time on the adsorption of Cr(VI) by adsorbents

Reaction duration has an impact on Cr(VI) adsorption, as shown in Fig. 3c, which displays greater Cr(VI) adsorption as reaction time increases. The elimination rate increased quickly between 0 and 180 minutes. The first adsorbent immediately bonded with Cr(VI) ions because its adsorption site was unbound. In the initial hours, the elimination of AC happens quickly, and 180 minutes later, equilibrium is reached. This suggests that Cr adsorption occurs in two stages: a phase of slow adsorption is followed by a phase of extremely rapid Cr adsorption. Adsorption owing to AC is greater than that of BC, as seen in Fig. 3c. The removal rate of BC can only be 38.50%. AC has a removal rate of 50% at 50 mg/L of Cr (VI) concentration.

Effect of temperatures for Cr(VI) removal by adsorbents

The impact of AC and BC adsorption of Cr(VI) at different temperatures and Cr(VI) concentrations is displayed in Fig. 3d. Up to 50% of the 50 mg/L Cr(VI) solution can be adsorbed. The

Figure 3: Effect of pH (a), Adsorbent dose (b), Effect of time on adsorption of Cr(VI) by BC and AC (c) Effect of temperature on adsorption of Cr(VI) by BC and AC (d)

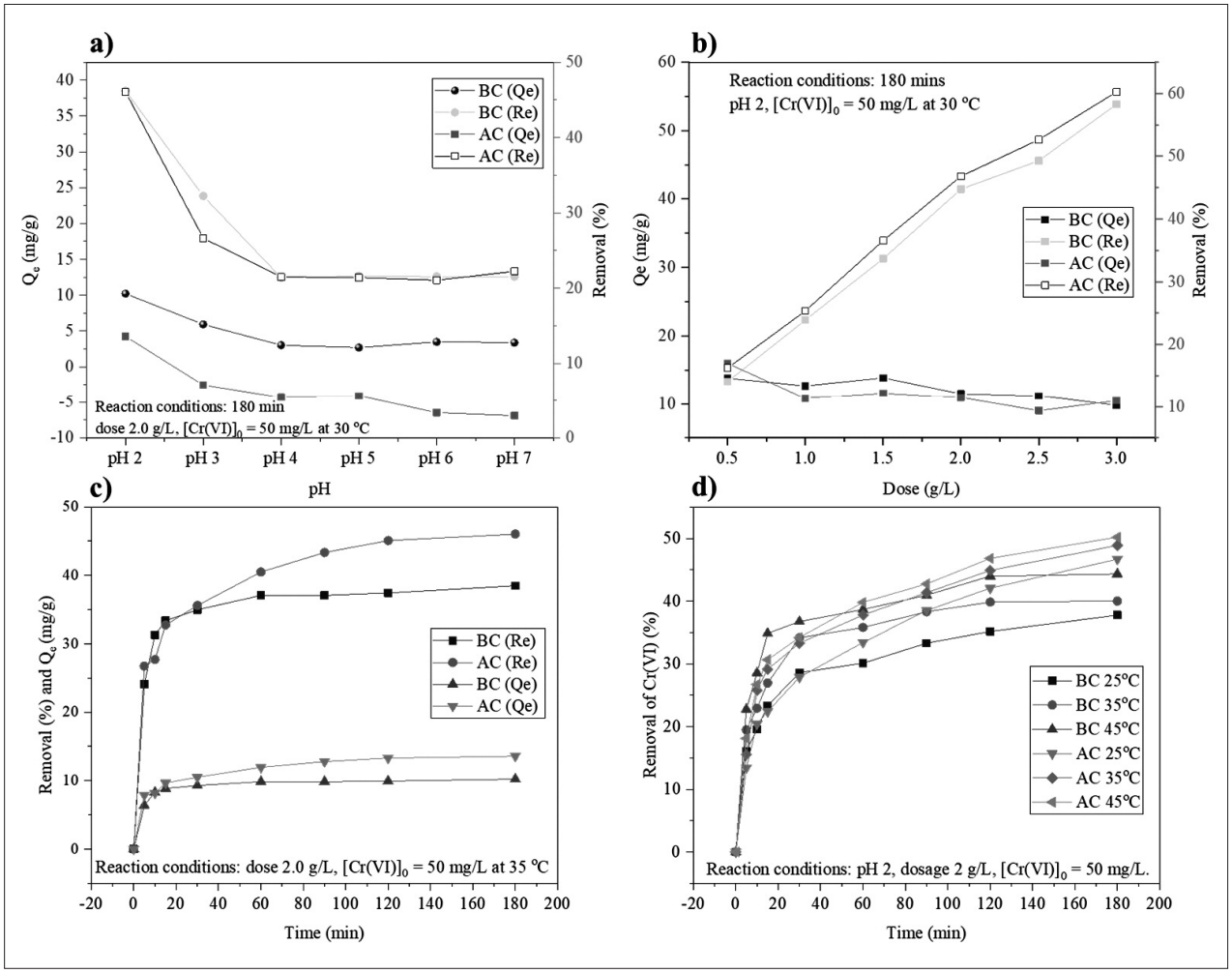

Source: Analysis by author

adsorption amount rises in tandem with the concentration, but the removal rate progressively falls [32]. The ideal temperature for the removal of aqueous Cr(VI) was indicated by the removal rate and adsorption capacity of the 50 mg/L Cr(VI) solution, which were at their peak at 45°C. The adsorption capacity of Cr(VI) has not been significantly affected by additional temperature increases.

3.4. Adsorption kinetics

In this study, the non-linearized form of reaction kinetic models was utilized to describe the experiment data, including the pseudo-first-order (PFO) and pseudo-second-order (PSO) model, the details are expressed in equation (3)-(4), respectively [33].

$$q_t = q_e(1-e^{-k_1 t}) \quad (3)$$

$$q_t = \frac{q_e^2 k_2 t}{1 + k_2 q_e} \quad (4)$$

Where

k1 (1/min) and k_2 (g/mg × min) are the rate constants of the PFO and PSO models, respectively;

q_e and q_t are the mount off Cr(VI) adsorbed at equilibrium and given time t (min), respectively.

Table 2 shows that in two different reaction models, AC had a better fitting degree than BC. A chemical reaction predominates during the

Table 2. Kinetic parameters of Cr(VI) adsorption onto BC and AC

Materials		BC	AC
		50 mg/L	50 mg/L
1. PFO model			
q_e	mg/g	10.27	11.20
k_1	1/min	0.098	0.078
R^2	-	0.938	0.963
2. PSO model			
q_e	mg/g	11.15	12.56
k_2	g/mg × min	0.013	0.008
R^2	-	0.979	0.991

Source: Analysis by author

Table 3. Isotherm parameters at 45°C of Cr(VI) adsorption onto BC and AC

Materials		BC	AC
1. Langmuir model			
Q_{max}	mg/g	99.64	319.13
K_L	L/mg	0.00148	6.23 × 10-4
R^2	-	0.969	0.978
2. Freundlich model			
n_F	-	1.423	1.193
K_F	(mg/g)/(mg/L)n	0.544	0.361
R^2	-	0.988	0.986

Source: Analysis by author

adsorption process, and activated carbon adsorbs Cr(VI), according to the PSO model's R^2 value (R^2 > 0.99), which is greater than the PFO model when compared to the R^2 value of the AC PFO model. It could happen via ion exchange, surface complexation, or electrostatic contact [34].

3.5. Adsorption isotherms

For adsorption isotherm, three adsorption models were used to demonstrate the interactive behavior between materials and Cr(VI) residues, including the Langmuir (5) and Freundlich (6) models [35].

$$q_t = \frac{q_{max} K_L C_e}{1 + K_L C_e} \quad (5)$$

$$q_e = K_F C_e^{1/n} \quad (6)$$

Where

Q_{max} (mg/g) is the Langmuir maximum adsorption capacity of absorbents;

K_L (L/mg) is the Langmuir constant related to the affinity between absorbents and Cr(VI);

K_F ((mg/g)/(mg/L)n) is the Freundlich constant, which characterizes the strength of adsorption;

n_F (dimensionless; 0<n<1) is a Freundlich intensity parameter, which indicates the magnitude of the adsorption driving force or surface heterogeneity.

The Freundlich and Langmuir isotherm models for the BC and AC adsorption of Cr(VI) at 45°C are shown in Table 3, along with the isotherm parameters. In both the Langmuir and Freundlich models, the R^2 value is greater than 0.9, indicating that both materials absorb the Cr(VI). The concepts of physical adsorption and chemisorption are applied during the procedure. Since the Freundlich model's n-value is larger than 1, AC is a superior adsorbent for Cr(VI) [36].

4. Conclusions

The results indicate that Cr(VI) adsorption by AC was superior to that by BC. At 45°C, pH = 2, and 50 mg/L of adsorption dose, the ideal conditions for adsorption are present. The surface element has successfully stuck to the P element, as confirmed by the modification in the pore density and surface area of AC as shown by SEM and EDS. This is advantageous to the Cr(VI) adsorption by the adsorbent and follows the pseudo-second-order kinetics. Chemistry and physics come together in the Cr(VI) adsorption process by AC ■

Acknowledgment:

The author would like to greatly acknowledge the support of time and facilities from the University of Technology, Vietnam National University - Ho Chi Minh City for this study.

REFERENCES:

1. R. N. Khalef, A. I. Hassan, and H. M. Saleh (2022). Heavy metal's environmental impact Environmental Impact and Remediation of Heavy Metals. Available at: https://doi.org/10.5772/intechopen.103907

2. G. Genchi, G. Lauria, A. Catalano, A. Carocci, and M. S. Sinicropi (2021). The double face of metals: The intriguing case of chromium Applied Sciences. Available at: https://doi.org/10.3390/app11020638

3. W. Jadaa and H. Mohammed (2023). Heavy metals–definition, natural and anthropogenic sources of releasing into ecosystems, toxicity, and removal methods–an overview study Journal of Ecological Engineering. Available at: https://doi.org/10.12911/22998993/162955

4. E. Vaiopoulou and P. Gikas (2020). Regulations for chromium emissions to the aquatic environment in Europe and elsewhere Chemosphere. Available at: https://doi.org/10.1016/j.chemosphere.2020.126876

5. L. He, T. He, S. Farrar, L. Ji, T. Liu, and X. Ma (2017). Antioxidants maintain cellular redox homeostasis by elimination of reactive oxygen species Cellular Physiology Biochemistry. Available at: https://doi.org/10.1159/000485089

6. W. H. Organization (2019). The WHO special initiative for mental health (2019-2023): universal health coverage for mental health.

7. A. Monga, A. B. Fulke, and D. Dasgupta (2022). Recent developments in essentiality of trivalent chromium and toxicity of hexavalent chromium: implications on human health and remediation strategies Journal of Hazardous Materials Advances. Available at: https://doi.org/10.1016/j.hazadv.2022.100113

8. B. E. Oyinloye, A. F. Adenowo, and A. P. Kappo (2015). Reactive oxygen species, apoptosis, antimicrobial peptides and human inflammatory diseases Pharmaceuticals. Available at: https://doi.org/10.3390/ph8020151

9. P. Carrott and M. R. Carrott (2007). Lignin–from natural adsorbent to activated carbon: a review Bioresource technology. Available at: https://doi.org/10.1016/j.biortech.2006.08.008

10. M. M. Sabzehmeidani, S. Mahnaee, M. Ghaedi, H. Heidari, and V. A. Roy (2021). Carbon based materials: a review of adsorbents for inorganic and organic compounds Materials Advances. Available at: https://doi.org/10.1039/D0MA00087F

11. P. Swaminaathan, A. Saravanan, and P. Thamarai (2024). Utilization of bioresources for high-value bioproducts production: Sustainability and perspectives in circular bioeconomy Sustainable Energy Technologies Assessments. Available at: https://doi.org/10.1016/j.seta.2024.103672

12. R. E. Sims (2003). Bioenergy options for a cleaner environment: in developed and developing countries Elsevier.

13. I. F. Demuner, J. L. Colodette, A. J. Demuner, and C. M. Jardim (2019). Biorefinery review: Wide-reaching products through kraft lignin BioResources. Available at: https://doi.org/10.15376/biores.14.3.Demuner

14. C.-H. Hsiao, S. Gupta, C.-Y. Lee, and N.-H. Tai (2023). Effects of physical and chemical activations on the performance of biochar applied in supercapacitors Applied Surface Science. Available at: https://doi.org/10.1016/j.apsusc.2022.155560

15. D. Azad, R. Pateriya, and R. K. Sharma (2021). A Review on Preparation and Characterization of Activated Bio - Char International Journal of Environment Climate Change. Available at: https://doi.org/10.9734/ijecc/2021/v11i430398

16. N. S. Lopa, B. N. Bhadra, N. A. Khan, S. Zhuiykov, and M. M. Rahman (2023). KOH/NaOH activated Carbon Biomass Based Supercapacitors: Design, Fabrication Sustainability. Available at: https://doi.org/10.1002/9781119866435.ch10

17. S. S. Shah, A. Aziz, L. Zada, H. U. Rahman, F. Niaz, and K. Hayat (2023). Carbonate Salts activated Carbon Biomass Based Supercapacitors: Design, Fabrication Sustainability. Available at: https://doi.org/10.1002/9781119866435.ch9

18. Z. Wang, D. Shen, C. Wu, and S. Gu (2018). State-of-the-art on the production and application of carbon nanomaterials from biomass Green Chemistry. Available at: https://doi.org/10.1039/C8GC01748D

19. Z. Yang, R. Gleisner, D. H. Mann, J. Xu, J. Jiang, and J. Zhu (2020). Lignin based activated carbon using H_3PO_4 activation Polymers. Available at: https://doi.org/10.3390/polym12122829

20. Y. Chen, S.-R. Zhai, N. Liu, Y. Song, Q.-D. An, and X.-W. Song (2013). Dye removal of activated carbons prepared from NaOH-pretreated rice husks by low-temperature solution-processed carbonization and H_3PO_4 activation Bioresource technology. Available at: https://doi.org/10.1016/j.biortech.2013.07.002

21. S. Penczek, J. Pretula, P. Kubisa, K. Kaluzynski, and R. Szymanski (2015). Reactions of H_3PO_4 forming polymers. Apparently simple reactions leading to sophisticated structures and applications Progress in Polymer Science. Available at: https://doi.org/10.1016/j.progpolymsci.2015.01.001

22. M. Danish and T. Ahmad (2018). A review on utilization of wood biomass as a sustainable precursor for activated carbon production and application Renewable Sustainable Energy Reviews. Available at: https://doi.org/10.1016/j.rser.2018.02.003

23. G. Chu, J. Zhao, Y. Huang, D. Zhou, Y. Liu, M. Wu, H. Peng, Q. Zhao, B. Pan, and C. E. Steinberg (2018). Phosphoric acid pretreatment enhances the specific surface areas of biochars by generation of micropores Environmental Pollution. Available at: https://doi.org/10.1016/j.envpol.2018.04.003

24. S. A. Dhar, T. U. Sakib, and L. N. Hilary (2022). Effects of pyrolysis temperature on production and physicochemical characterization of biochar derived from coconut fiber biomass through slow pyrolysis process Biomass Conversion Biorefinery. Available at: https://doi.org/10.1007/s13399-020-01116-y

25. K. Dujearic-Stephane, M. Gupta, A. Kumar, V. Sharma, S. Pandit, P. Bocchetta, and Y. Kumar (2021). The effect of modifications of activated carbon materials on the capacitive performance: surface, microstructure, and wettability Journal of Composites Science. Available at: https://doi.org/10.3390/jcs5030066

26. C. Duan, T. Ma, J. Wang, and Y. Zhou (2020). Removal of heavy metals from aqueous solution using carbon-based adsorbents: A review Journal of Water Process Engineering. Available at: https://doi.org/10.1016/j.jwpe.2020.101339

27. U. O. Aigbe and O. A. Osibote (2020). A review of hexavalent chromium removal from aqueous solutions by sorption technique using nanomaterials Journal of Environmental Chemical Engineering. Available at: https://doi.org/10.1016/j.jece.2020.104503

28. O. Njoya, S. Zhao, Y. Qu, J. Shen, B. Wang, H. Shi, and Z. Chen (2020). Performance and potential mechanism of Cr (VI) reduction and subsequent Cr (III) precipitation using sodium borohydride driven by oxalate Journal of Environmental Management. Available at: https://doi.org/10.1016/j.jenvman.2020.111165

29. I. Apostol, N. Anghel, F. Doroftei, A. Bele, and I. Spiridon (2023). Xanthan or esterified xanthan/cobalt ferrite-lignin hybrid materials for methyl blue and basic fuchsine dyes removal: equilibrium, kinetic and thermodynamic studies Materials Today Chemistry. Available at: https://doi.org/10.1016/j.mtchem.2022.101299

30. S. Singh, D. Kapoor, S. Khasnabis, J. Singh, and P. C. Ramamurthy (2021). Mechanism and kinetics of adsorption and removal of heavy metals from wastewater using nanomaterials Environmental Chemistry Letters. Available at: https://doi.org/10.1007/s10311-021-01196-w

31. A. Safonov, N. Popova, N. Andrushenko, K. Boldyrev, N. Yushin, and I. Zinicovscaia (2021). Investigation of materials for reactive permeable barrier in removing cadmium and chromium (VI) from aquifer near a solid domestic waste landfill Environmental Science Pollution Research. Available at: https://doi.org/10.1007/s11356-020-10743-x

32. T. C. Egbosiuba, A. S. Abdulkareem, A. S. Kovo, E. A. Afolabi, J. O. Tijani, M. T. Bankole, S. Bo, and W. D. Roos (2021). Adsorption of Cr (VI), Ni (II), Fe (II) and Cd (II) ions by KIAgNPs decorated MWCNTs in a batch and fixed bed process Scientific reports. Available at: https://doi.org/10.1038/s41598-020-79857-z

33. R. Ezzati (2020). Derivation of pseudo-first-order, pseudo-second-order and modified pseudo-first-order rate equations from Langmuir and Freundlich isotherms for adsorption Chemical Engineering Journal. Available at: https://doi.org/10.1016/j.cej.2019.123705

34. A. E. Ofomaja, E. B. Naidoo, and A. Pholosi (2020). Intraparticle diffusion of Cr (VI) through biomass and magnetite coated biomass: A comparative kinetic and diffusion study South African Journal of Chemical Engineering. Available at: https://hdl.handle.net/10520/EJC-1d7a4c6819

35. S. Mouhamadou, S. Dalhatou, N. Dobe, R. Djakba, O. O. Fasanya, N. D. Bansod, G. Fita, C. H. Ngayam, J. P. Tejeogue, and M. Harouna (2023). Linear and non-linear modelling of kinetics and equilibrium data for Cr (VI) adsorption by activated carbon prepared from Piliostigma reticulatum Chemistry Africa. Available at: https://doi.org/10.1007/s42250-022-00324-5

36. S. Acharya, S. Sahoo, S. Sonal, J. H. Lee, B. K. Mishra, and G. Nayak (2020). Adsorbed Cr (VI) based activated carbon/polyaniline nanocomposite: a superior electrode material for asymmetric supercapacitor device Composites Part B: Engineering. Available at: https://doi.org/10.1016/j.compositesb.2020.107913.

Received date: July 25, 2024
Reviewed date: August 7, 2024
Accepted date: August 19, 2024

Author's information:
DANG VIET HUNG
Faculty of Environment and Natural Resources
University of Technology, Vietnam National University -Ho Chi Minh City

ỨNG DỤNG THAN HOẠT TÍNH TỪ XƠ DỪA LOẠI BỎ CROM (VI)

● **ĐẶNG VIẾT HÙNG**
Khoa Môi trường và Tài nguyên, Trường Đại học Bách khoa
Đại học Quốc gia Thành phố Hồ Chí Minh

TÓM TẮT:

Than sinh học được coi là một môi trường hấp phụ kinh tế do khả năng loại bỏ kim loại nặng và các chất ô nhiễm hữu cơ từ nước ô nhiễm. Trong nghiên cứu này, axit photphoric (H_3PO_4) đã được sử dụng theo cách độc đáo để thúc đẩy quá trình sản xuất than hoạt tính từ sợi dừa (AC) từ carbon biochar (BC) thông qua quá trình nhiệt phân. Sản phẩm thu được sau đó đã được thử nghiệm khả năng hấp phụ hiệu quả Cr (VI) từ môi trường nước. Để đánh giá cấu trúc và thành phần của BC và AC, các kỹ thuật đặc trưng tiên tiến như SEM, EDS, và pHpzc đã được sử dụng. So với tỷ lệ loại bỏ Cr(VI) của BC là 38,5%, AC có thể loại bỏ 48,05% Cr(VI). Các yếu tố sau đây có ảnh hưởng đáng kể đến tỷ lệ loại bỏ Cr(VI): nhiệt độ, động học, đẳng nhiệt, thời gian hấp phụ, pH và khả năng hấp phụ. Đường cong hấp phụ của AC phù hợp tốt với mô hình động học bậc hai giả.

Từ khóa: khử Cr (VI), than hoạt tính, xơ dừa, hấp phụ, acid photphoric.